



Suprathermal LPIC++ Model for Laser Plasma Acceleration

Djemai Bara, El-Hadj Dahi and Djamila Bennaceur-Doumaz

EasyChair preprints are intended for rapid dissemination of research results and are integrated with the rest of EasyChair.

March 23, 2021

Suprathermal LPIC++ Model for Laser Plasma Acceleration

Djemai Bara^{1*}, El-Hadj Dahi², Djamila Bennaceur-Doumaz¹

Abstract

In the aim of researching and interpreting energy spectra and maximum energies of protons accelerated by ultra-intense and ultra-short laser pulses, authors have proposed simulations, assuming Maxwellian distributions for the electrons. Nevertheless, it is well known that electrons ejected during interaction of a high intensity laser with a solid target, responsible for proton acceleration, are nonthermally distributed inside the created plasma. In this work, one-dimensional Particle-In-Cell calculations using LPIC++ simulation code were established in the framework of Target Normal Sheath Acceleration "TNSA". The prepulse laser CPA (Chirped Pulse Amplification) has an intensity $\sim 10^{12} \text{ W/cm}^2$ and a duration $\sim \text{ns}$, which creates a primary slab of plasma with nonthermal electrons, governed by a discretized kappa electron distribution function. The following main pulse has an intensity $\sim 10^{18} \text{ W/cm}^2$ and a duration $\sim \text{fs}$. By varying the intensities of the main pulse, the initial plasma species distribution and the nonthermal parameter kappa, the proposed model shows an enhancement in the different acceleration features in the TNSA mechanism compared to those deduced from Maxwellian simulation models. This study is useful in applications involving the creation of energetic ion beams, such as protontherapy.

Keywords

Laser plasma acceleration — TNSA — Kappa electron distribution function

¹ Centre de Développement des Technologies Avancées, B.P. 17 Baba Hassen 16303 Algiers, Algeria.

² Laboratoire de Physique Théorique, Abou Beker Blekaid University, Tlemcen, Algeria.

* Corresponding author: dbara@cdda.dz, djemaibara@gmail.com

Introduction

Recently, ion laser-acceleration using ultra intense, short laser pulses in interaction with overdense plasmas where multi-MeV, quasi-mono energetic, collimated protons beams are produced [1], has attracted considerable interest. Indeed, these beams are useful for many applications such as inertial confinement fusion (ICF), radiation therapy [2], isotope production [3-5], etc. The ion beams are generated via different acceleration mechanisms, particularly via Target Normal Sheath Acceleration (TNSA). The process is based essentially on the interaction of a CPA (Chirped Pulse Amplification) [6] laser with a solid target. First, a laser prepulse generates a pre-plasma at the front of the target, followed by the arrival of the main pulse which creates energetic hot electrons. These electrons are transported into the target, ionizing the rear surface, creating then plasma where ions are pulled off the surface and accelerated to tens of MeVs, in few μms .

To deepen the understanding of the physical phenomena that contribute to the control of the ion beams, great importance has been given to the modeling and simulations of these electrons, responsible for the ionic acceleration, via the electric field induced by charge separation. In fact, in the laser matter interaction experiments, it has been shown that the first created electrons are fast, noncollisional then

their distribution functions are nonthermal with high velocity tails; the presence of these electrons is an important condition to generate energetic protons in TNSA laser driven proton acceleration [7, 8]. In plasma expansion into vacuum, it is proved that assuming an initial non-Maxwellian distribution function of the energetic electrons leads to an important enhancement of ion energies up to an order of magnitude from the values obtained with the Maxwellian case. Particularly, suprathermal electron distribution functions have been already used by many authors to simulate the nonthermal effects on the ion acceleration process [9].

In the present work, PIC simulations are performed using one-dimensional fully relativistic kinetic 1D3V LPIC++ [10], to study the interaction of a varying intensity laser pulse with initially suprathermal slab of plasma where electrons are obeying kappa distribution with different κ values, in the framework of TNSA acceleration process. For that, a modification in the code has been performed to generate an initial kappa distribution function for the energetic electrons, in order to optimize the suprathermal parameter value that allows having quasi-monoenergetic ion acceleration, with large proton beam energies, as it is required by many applications, such as protontherapy.

1. Simulation model

In this paper, for studying laser slab plasma interaction, a 1D3V LPIC++ collisionless fully relativistic electromagnetic Particle-In-Cell simulation code is used [10]. The simulation box dimension is $320 \mu\text{m}$, with 4000 cells. The slab of plasma is initially located in the center of the simulation box. Its size is $40 \mu\text{m}$, containing 20000 particles per cell. The initial density plasma n is normalized to the critical density n_c , such as $n = 10n_c$ where $n_c = \omega^2(m_e \epsilon_0 / e^2)$; ω , m_e , e and ϵ_0 denote the laser frequency, the mass of electron at rest, the charge of electron and vacuum permittivity, respectively. The laser wavelength is $\lambda = 0.8 \mu\text{m}$ and its pulse duration is 35 fs. The propagation of the laser pulse with s-polarization begins from the left of the simulation box, perpendicularly to the initial plasma slab.

To include electron nonthermal effects on the dynamics of plasma and proton acceleration process, the code has been modified by introducing an initial discretized kappa electron distribution function in the simulation model. The implementation of the kappa distribution in the code is done using the generation of random number.

The kappa electron distribution functions for various suprathermal parameter values are given by the equation (1).

$$f_e = \frac{n_{e0}}{\sqrt{\pi}} + \frac{1}{\theta \kappa^2} + \frac{\Gamma(\kappa+1)}{\Gamma(\kappa-\frac{1}{2})} + \left(1 + \frac{v_e^2}{\kappa \theta^2}\right)^{-\kappa} \quad (1)$$

Where $\theta = (2\kappa - 3/\kappa)^{1/2} (T_e/m_e)^{1/2}$ is the average electron thermal energy.

n_{e0} , v_e , and T_e are the density at rest, the velocity, and the temperature of the electrons, respectively. $\kappa \geq 3/2$ is the nonthermal parameter which measures the deviation from the maxwellian case. For $\kappa \rightarrow \infty$, we obtain the maxwellian distribution function at the equilibrium state:

$$f_e = \frac{n_{e0}}{\sqrt{\pi}} \frac{1}{\theta} \exp\left(-\frac{v_e^2}{\theta^2}\right), \quad \theta = \left(\frac{2T_e}{m_e}\right)^{1/2} \quad (2)$$

2. Results and Discussion

We are interested in protons acceleration in the rear face of laser irradiated plasma slab in the framework of the TNSA mechanism. The present model supposes a creating slab plasma with initially kappa distributed electrons having varying κ parameter values. The laser pulse intensity in our simulation ranges between 1.92×10^{19} and $7.7 \times 10^{19} \text{W/cm}^2$ corresponding to the laser field amplitude $a_0 = eE_0/m_e \omega c$, between 3 and 6, where, E_0 is the initial laser electric field amplitude and c is the light celerity.

To study the influence of both effects of suprathermality (represented by κ) and laser intensity (represented by a_0) on proton acceleration, we have

plotted the evolution of spatial proton density profiles, energy spectra, spatio-temporal electric fields, proton phase spaces, the maximum proton energies and proton front positions as function of a_0 .

2.1. Proton energy spectra

In Figure 1, we have illustrated the energy spectra of the protons as a function of their energies for $t = 1000T$ and for different laser intensity a_0 and κ values. As a result, with the increasing of the suprathermal number electrons (κ decreasing), the number of protons per energy unit is increasing, for instance, for $a_0 = 5$, a maximum of proton energy is obtained at the end of expansion for all the profiles of energy spectra depending also on nonthermal and intensity laser effects. The maximum proton energies are more important when a_0 and nonthermal effects are important.

As examples, for $\kappa = 3$, a maximum of proton energy of 21.3 MeV is obtained for laser intensity parameter $a_0 = 3$, an energy of 22.4 MeV for $a_0 = 4$, an energy of 23.3 MeV, for $a_0 = 5$ and 24.4 MeV for $a_0 = 6$.

In the case of near Maxwellian electron distribution ($\kappa = 10$, Fig. 1. (d)), a maximum of proton energy of 14.8 MeV is obtained for laser intensity parameter $a_0 = 3$, 16.5 MeV for $a_0 = 4$, 18.4 MeV for $a_0 = 5$ and, 23.3 MeV for $a_0 = 6$.

To better show the nonthermal effects, in Figure 2, for a given laser intensity $a_0 = 3$, the number of protons N per energy unit is increasing with nonthermal effects. For instance, for $\kappa = 10$, $N = 19$, $\kappa = 6$, $N = 30$, $\kappa = 4$, $N = 37$ and $\kappa = 3$, $N = 53$ at a proton energy $E = 12 \text{MeV}$.

2.2. The electric field

A spatio-temporal evolution of the longitudinal electric fields E_x for various values of laser intensities and initial suprathermal electronic populations, is schematized in Figure 3. It is seen that the electric field rises when both nonthermality and laser field amplitude increase, because the induced charge separation becomes more significant in the TNSA mechanism at the rear surface into vacuum. This is due to the initial flux of suprathermal energetic electrons which extend the electrostatic field further spatially and enhance its intensity (see Fig. 4). Therefore, the proton beam gains more energy and acceleration.

2.3. The ion velocities

The two figures 4 and 5 show longitudinal and transverse phase spaces, respectively, in the case of the presence of suprathermal electrons population with $\kappa = 3$ and for $a_0 = 3, 4$, and 5 (Figs. 4, 5(a1), (b1) and (c1)) and in the case of maxwellian electrons for $a_0 = 3, 4$, and 5 (Figs. 4, 5(a2), (b2) and (c2)) at time $t = 800T$.

In the absence of nonthermal effects (Maxwellian electrons) in the plasma expansion, it is only the influence of laser intensity that is shown in Figures

5(a2), (b2) and (c2). In fact, the longitudinal proton velocity is increasing and the number of accelerated protons is greater when the laser intensity is increasing (a_0 is increasing) and the acceleration process is kept further spatially (in accordance with Fig. 1). In the

other hand, the same behavior is noticed in the Figures 5(a1), (b1) and (c1), where the nonthermal effects are present and important ($\kappa=3$).

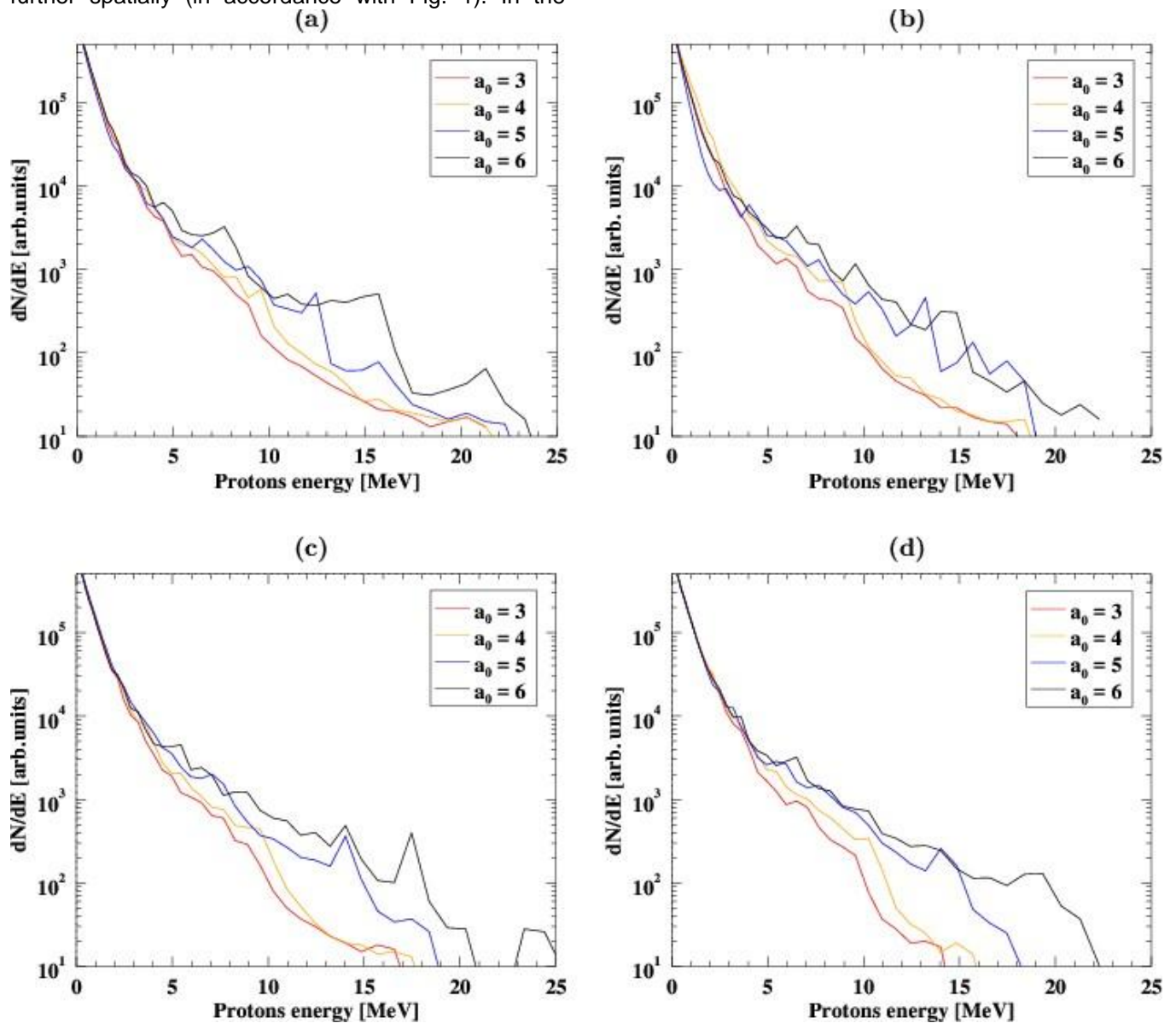


Figure 1. Energy spectra as function of proton energy with different laser intensities (a_0) at $t = 1000T$ for $\kappa = 3$ (a), $\kappa = 4$ (b), $\kappa = 6$ (c) and $\kappa = 10$ (d)

We also noticed that for a fixed a_0 , nonthermal effects enhance proton acceleration comparatively to the Maxwellian case, while in Figures 5(a1), (b1) and (c1), we observe the appearance of a transverse velocity tail of the protons located far from the target, due to the small number of transversely accelerated

protons for $\kappa=3$ comparatively to the case of Maxwellian distribution (Figs. (a2), (b2) and (c2)). Consequently, the accelerated proton beam is more collimated (less divergent) when there is a large deviation from the Maxwellian electron distribution ($\kappa=3$). This decrease in the proton beam divergence is also

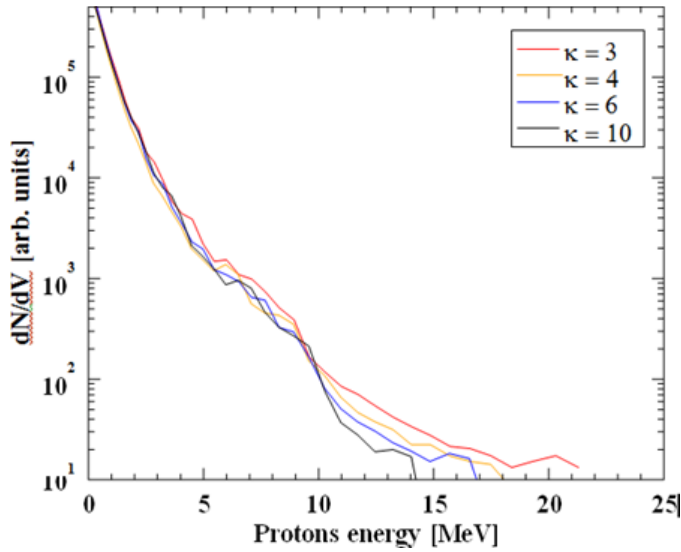


Figure 2. Energy spectra as function of proton energy with different values of (κ) at $t=1000T$ for $a_0=3$.

more pronounced with increasing a_0 . The proton phase space at $t = 800T$ shows that an accumulated set of protons appears far from the target rear surface.

In fact, when the population of the suprathermal electrons is increasing, (decreasing κ), the accelerated proton front is expanding further, while this effect becomes less efficient for great laser intensities a_0 . Imposing initial suprathermal electrons in the slab of plasma before the arrival of the intense laser pulse, in the simulation model, is similar to the experiments where double intense laser pulses are involved in laser plasma interaction. The main objective in these experiments is to improve the mechanism of hot electrons ejection from the target, which enhances the number of energetic electrons and their energies, leading to the increase of the laser pulse absorption, this is done by replacing the laser pre-pulse ($I \sim 10^{12} W/cm^2$, $\tau \sim ns$) in the CPA technique by a first intense laser pulse ($I \sim 10^{16} W/cm^2$, $\tau \sim fs$).

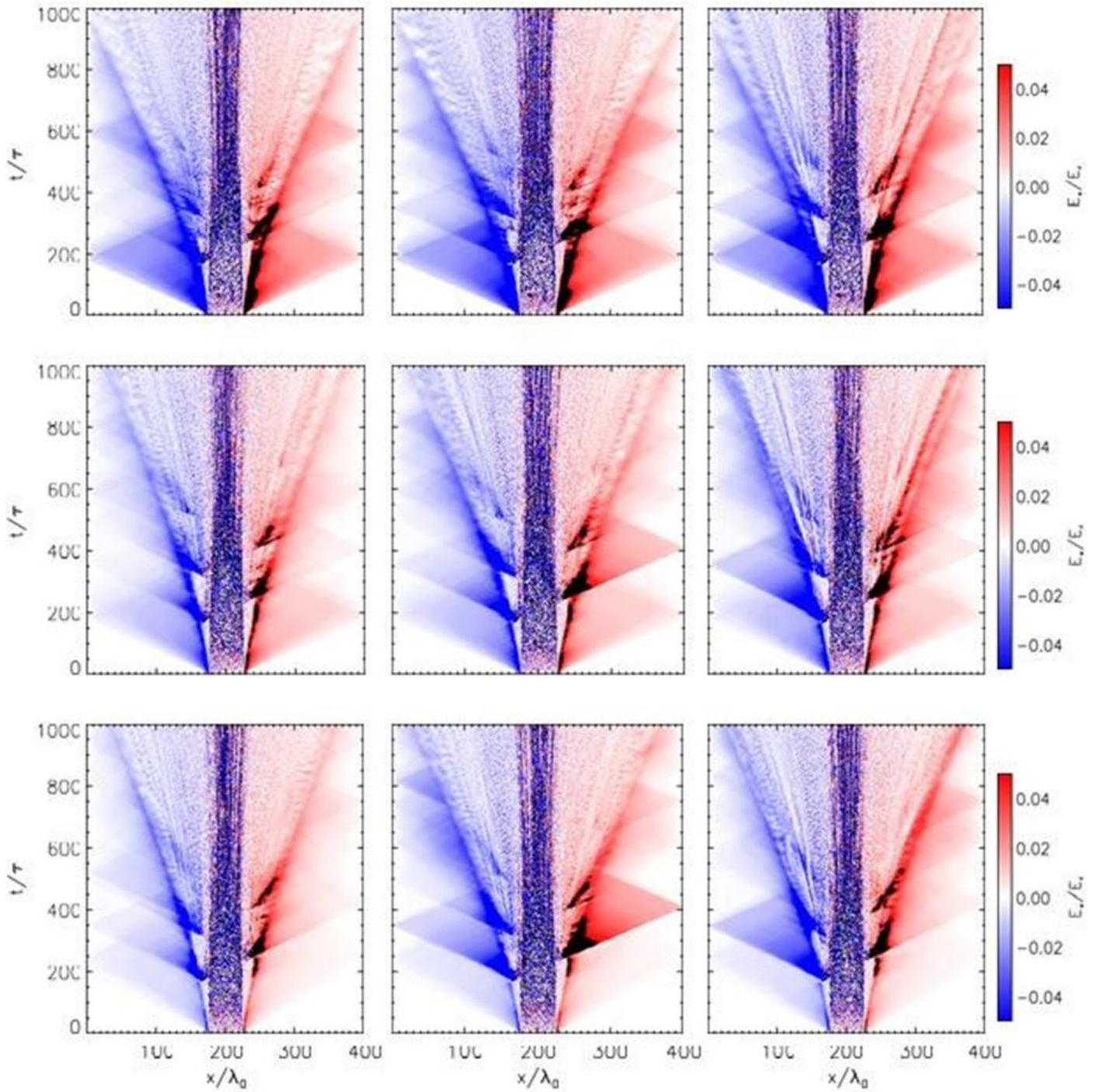


Figure 3. Spatio-temporal evolution of the normalized longitudinal electric field (E_x), for $\kappa = 3$ and $a_0 = 3, 4, 5$, Figs. a1, a2, a3, respectively, for $\kappa = 10$ and $a_0 = 3, 4$, and 5 , Figs. b1, b2, b3, respectively and for Maxwellian electron distribution and $a_0 = 3, 4$ and 5 , Figs. c1, c2, c3, respectively.

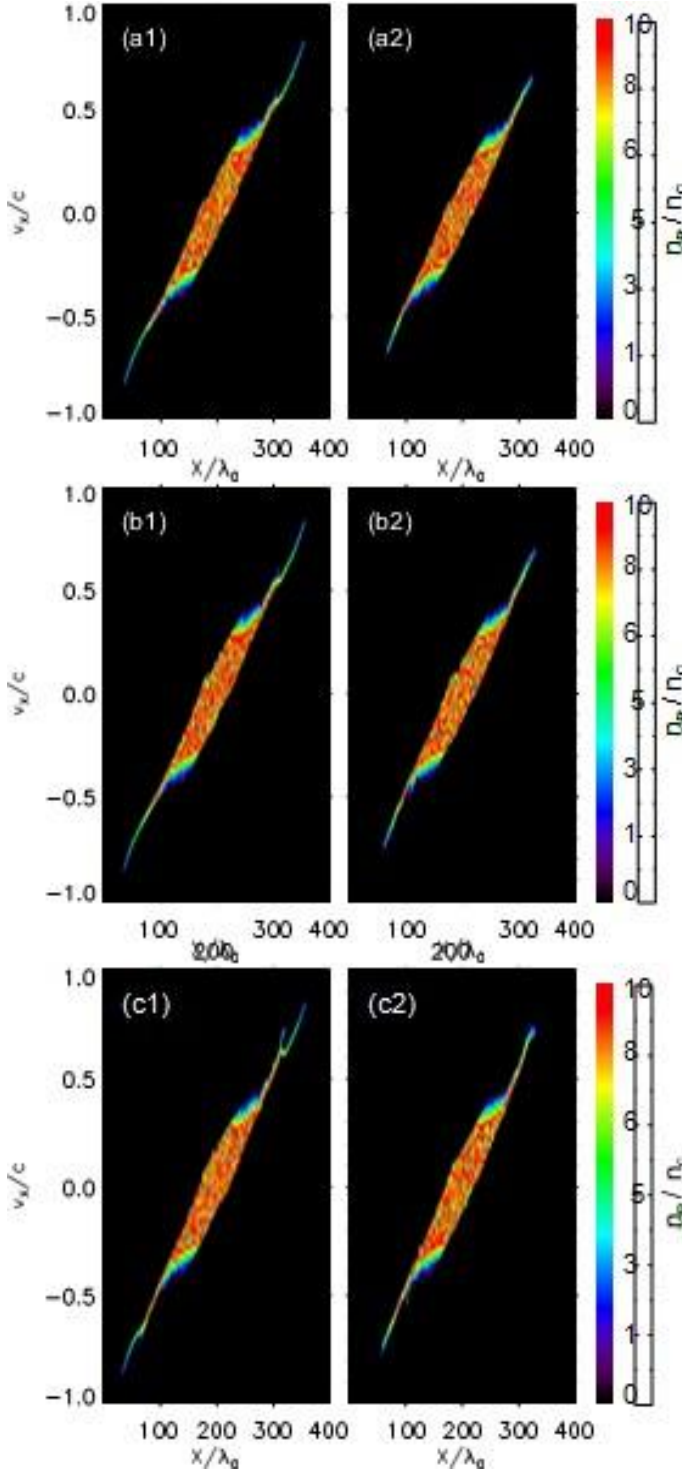


Figure 4. Proton longitudinal velocities (v_x) at $t=800T$, for $\kappa = 3$ with $a_0 = 3, 4,$ and 5 Figs . (a1),(b1) and (c1); and Maxwellian electrons with $a_0 = 3, 4,$ and 5 Fig . (a2), (b2) and (c2).

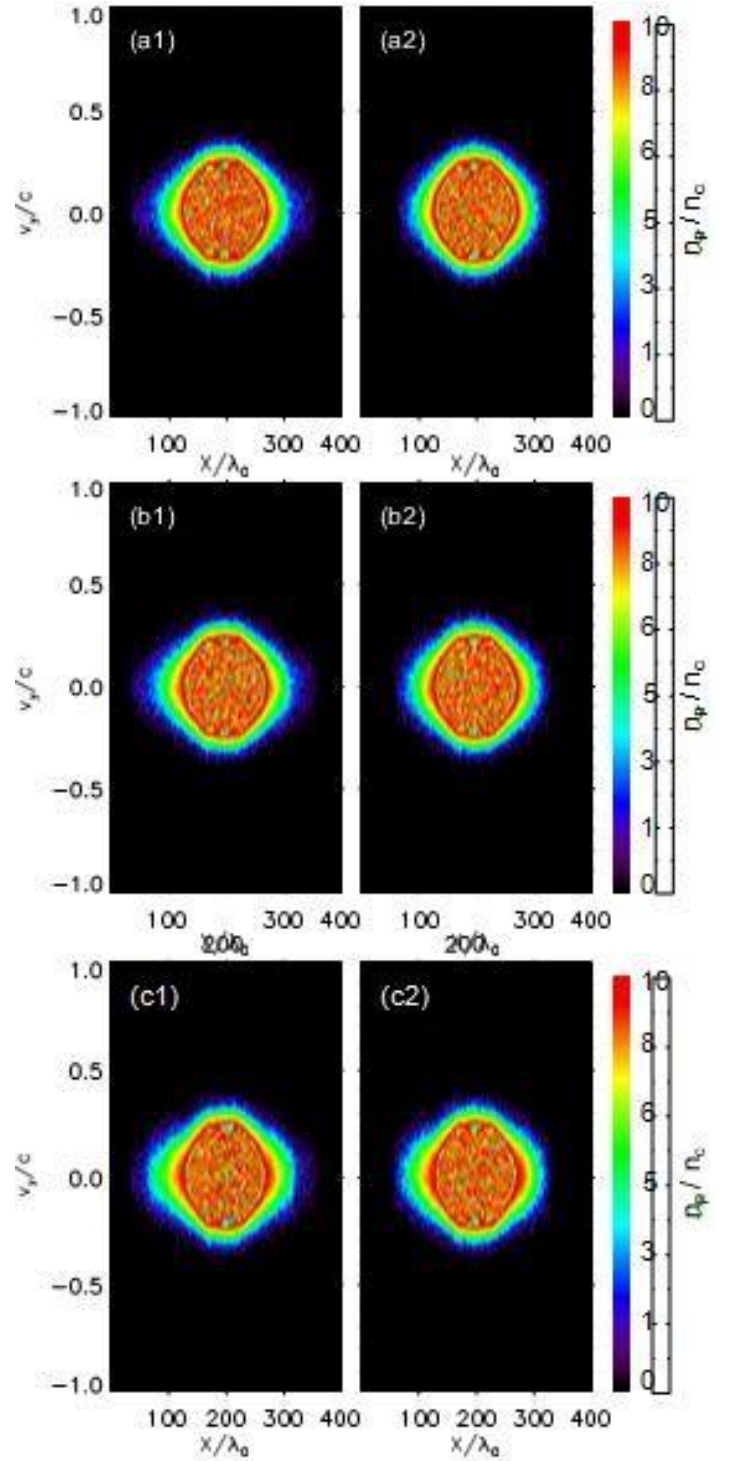


Figure 5. Normalized proton transversal velocities (v_y) at $t=800T$, for $\kappa = 3$ with $a_0 = 3, 4,$ and 5 Figs (a1),(b1) and (c1); and Maxwellian electrons with $a_0 = 3, 4,$ and 5 (Figs (a2), (b2) and (c2)).

3. Conclusion

The present work concerns a PIC simulation study of the influence of varying laser pulse intensities on the expansion of plasma slab with initially kappa distributed electrons in the laser plasma acceleration phenomena. It has been shown that the proton acceleration in TNSA mechanism strongly depends on both the laser intensity and the presence of suprathermal electrons. It has been proved that the numbers of accelerated protons, their energies are more important and plasma expansion is more extended with increasing laser intensity and decreasing suprathermal κ parameter. Near the source, these two effects are negligible because the TNSA acceleration process via the electric field of charge separation did not take place. In the other hand, in the expanding plasma core, it is the laser effect which is more important. At the plasma expansion front, a strong electric field induced by large charge separation, caused by the suprathermal energetic electrons tail dominates the laser intensity effect. We also find that when there is a large deviation from the Maxwellian electron distribution and when the intensity of the laser is increasing, the accelerated proton beam is much less divergent. It turns out that this study presents an analogy with the experiments done with the interaction of double intense laser pulses with a plasma sheet in order to enhance the number of energetic electrons to better control proton beam acceleration. The physical interpretation of our simulation results allowed us to understand the experiments of ion acceleration in the laboratories and to focus on the importance of the accelerated beam applications for the fight against the cancer.

References

- [1] S. Bagchi, M. Tayyab, J. Pasley, A. P. L. Robinson, M. Nayak and J. A. Chakera. Quasi mono-energetic heavy ion acceleration from layered targets. *Physics of Plasmas*, 28:023108, 2021.
- [2] J. P. Gross, S. Y. Kim, V. Gondi, M. Pankuch, S. Wagner, A. Grover, Y. Luan and T. K. Woodruff. Proton Radiotherapy to Preserve Fertility and Endocrine Function. *Int. J. Radiation Oncol. Biol. Phys.*, 109:84-94, 2021.
- [3] R. Clarke, S. Dorkings, D. Neely, I. Musgrave. The production of patient dose level ^{99m}Tc medical radioisotope using laser-driven proton beams. *Proceedings, 8779, Laser Acceleration of Electrons, Protons, and Ions II; and Medical Applications of Laser-Generated Beams of Particles II; and Harnessing Relativistic Plasma Waves III; 87791C*, 2013.
- [4] A. K. Spiliotis, M. Xygkis, M. E. Koutrakis, K. Tazes, G. K. Boulogiannis, C. S. Kannis, G. E. Katsoprinakis, D. Sofikitis and T. P. Rakitzis : Ultrahigh-density spin-polarized hydrogen isotopes from the photodissociation of hydrogen halides, new applications for laser-ion acceleration, magnetometry, and polarized nuclear fusion. *Light Sci. Appl.*, 10:35, 2021.
- [5] P. Hill and Y. Wu. Exploring laser-driven neutron sources for neutron capture cascades and the production of neutron-rich isotopes. *Phys. Rev. C*, 103:014602, 2021.
- [6] D. Strickland and G. Mourou, Compression of amplified chirped optical pulses. *Optics Communications*, 56:219-221, 1985.
- [7] D. Bara, M. F. Mahboub and D. Bennaceur-Doumaz. Ion front acceleration in collisional nonthermal plasma. *Eur. Phys. J. D*, 74:224, 2020.
- [8] D. Bara, M. F. Mahboub and D. Bennaceur-Doumaz. Dynamic evolution of ionization and recombination processes and ion front acceleration in the presence of nonthermal and trapped electrons. *J. Phys.: Conf. Ser.*, 1766:012013, 2021.
- [9] D. Bennaceur-Doumaz and D. Bara. Self-similar solution of laser-produced plasma expansion into vacuum with kappa-distributed electrons. *Nukleonika*, 61:115-118, 2016.
- [10] R. Lichters, R.E.W. Pfund and J. Meyer-ter-Vehn, *LPIC++: A Parallel One-dimensional Relativistic Electromagnetic Particle-in-Cell Code for Simulating Laser-Plasma Interactions*, Rep. MPQ, 225: Max-Planck Institut für Quantenoptik, 1997.